



Asymmetric changes of temperature in the Arctic during the Holocene based on a transient run with the CESM

Hongyue Zhang^{1,2}, Jesper Sjolte^{2,*}, Zhengyao Lu³, Jian Liu^{1,4,5,*}, Weiyi Sun¹, Linfeng Wan⁶

¹ Key Laboratory for Virtual Geographic Environment, Ministry of Education, State Key Laboratory Cultivation Base of Geographical Environment Evolution of Jiangsu Province, Jiangsu Center for Collaborative Innovation in Geographical Information Resource Development and Application, School of Geography Science, Nanjing Normal University, Nanjing 210023, China

² Department of Geology – Quaternary Science, Lund University, Lund, 223 62, Sweden

³ Department of Physical Geography and Ecosystem Science, Lund University, Lund, 223 62, Sweden

⁴ Jiangsu Provincial Key Laboratory for Numerical Simulation of Large-Scale Complex Systems, School of Mathematical Science, Nanjing Normal University, Nanjing 210023, China

⁵ Open Studio for the Simulation of Ocean-Climate-Isotope, Qingdao National Laboratory for Marine Science and Technology, Qingdao 266237, China

⁶ Institute of Advanced Ocean Study, Ocean University of China, Qingdao, China

15 *Correspondence to:* Jesper Sjolte (jesper.sjolte@geol.lu.se), Jian Liu (jliu@njnu.edu.cn)

Abstract. The Arctic temperature changes are closely linked to midlatitude weather variability and extreme events, which has attracted much attention in recent decades. Syntheses of proxy data from poleward of 60°N indicate that there was asymmetric cooling of -1.54 °C and -0.61 °C for Atlantic Arctic and Pacific Arctic during the Holocene, respectively. We also present a similar consistent cooling pattern from an accelerated transient Holocene climate simulation based on the Community Earth System Model. Our results indicate that the asymmetric Holocene Arctic cooling trend is dominated by the winter temperature variability with -0.67 °C cooling for Atlantic Arctic and 0.09 °C warming for Pacific Arctic, which is particularly pronounced at the proxy sites. Our findings indicate that sea ice in the North Atlantic expanded significantly during the late Holocene, while a sea ice retreat is seen in the North Pacific, amplifying the cooling in the Atlantic Arctic by the sea ice feedback. The positive Arctic dipole pattern, which promotes warm southerly winds to the North Pacific, offsets parts of the cooling trend in Pacific Arctic. The Arctic dipole pattern also causes sea ice expansion in the North Atlantic, further amplifying the cooling asymmetry. We found that the temperature asymmetry is more pronounced in a simulation driven only by orbital forcing, indicating that the orbital modulation of the Pacific Decadal Oscillation, which in turn links to the Arctic dipole pattern, further affects the temperature asymmetry.

1 Introduction

30 Arctic climate is a critical component of the climate system. Since the 1990s, the changes in the Arctic climate have attracted increasing attention. Observational and model data show that the Arctic temperature variability is much greater than the global mean temperature variability, known as the Arctic amplification (AA) (Jones and Moberg, 2003; Holland and Bitz, 2003;



Serreze and Barry, 2011). The Intergovernmental Panel on Climate Change (IPCC, 2021) suggests that the Arctic temperature has likely increased more than double compared to the global average with high confidence over the last two decades. There has been intense debate about how the Arctic amplification (AA) affects the mid-latitude circulation, with some scholars suggesting that the AA increases the equator-to-pole temperature gradient and impacts the predominant westerly wind through the thermal-wind relation, which leads to disturbances in the mid-latitude circulation, further increasing the probability of extreme weather in the mid-latitudes (Smith et al., 2019; Vavrus, 2018; Screen and Simmonds, 2014; Cohen et al., 2014; Francis and Vavrus, 2012, 2015). The changes in Arctic temperature have also been directly linked to the sea ice loss or expansion, which affect the exchanges of heat and moisture between the ocean and atmosphere as well as the salinity of the ocean (Aagaard and Carmack, 1989; Wu et al., 2004; Goosse and Fichefet, 1999; Deser et al., 2016). Changes in sea ice extent and salinity in turn leads to changes in the thermohaline circulation (Rahmstorf, 1999; Alekseev et al., 2001), which may cause significant negative impacts on the climate and maritime transportation (Ragner, 2000) in high latitude regions. All these processes have strong impacts on the regional economic development.

The different drivers of the significant increase in temperature at high latitudes over the past decades have been debated by scholars, and it is widely accepted that one of the extremely important factors is the natural variability (Polyakov and Johnson, 2000; Polyakov et al., 2002; Delworth and Knutson, 2000). For the past decades, Hoerling et al. (2001) show that due to the increase in tropical temperature, convective activity has increased, resulting in an increase in the North Atlantic Oscillation/Arctic Oscillation (NAO/AO) positive pattern, which is significantly related with the Arctic temperature (Hurrell, 1995). Deser et al. (2015) and Blackport et al. (2018) attribute part of the warming of the Arctic to increasing in extratropical ocean temperature. Johannessen et al. (2004) used ECHAM4 and HadCM3 and found that the anthropogenic forcing is the dominant reason for the Arctic warming over the past decades. For the centennial and millennial time scales, the anomalies in summer insolation, driven primarily by Earth's orbital forcing, have a greater impact on the Arctic region than the low latitudes and amplify changes in temperature through positive feedbacks. Many scholars proposed a link between Arctic temperature trends and summer insolation changes, especially during the early-mid Holocene (Park et al., 2018; Marcott et al., 2013; Kaufman et al., 2009). Arctic temperature change affects the radiative balance, which dominates the surface energy balance that controls Arctic sea ice growth and melting (Kay et al., 2008; Francis and Hunter, 2007). At the same time, sea ice changes and trends affect Arctic temperature through feedbacks and also influence Arctic atmospheric circulation changes, particularly in the lower troposphere during winter (Barnes and Screen, 2015; Overland and Wang, 2015; Francis and Skific, 2015; Cohen, 2016). The Holocene proxy data also suggest that a decrease in the Arctic sea ice relative to the present, impacting the temperature gradient between equator and pole, which might enhance warming in North American and North Pacific regions, leading to a slight decrease in temperature over East Asia, and shifting tropical rainfall northwards (Smith et al., 2019; Park et al., 2018; Hanslik et al., 2010; Funder et al., 2011; Müller et al., 2012).

From a geological perspective the characterization of the Arctic temperature variability captured by observational data is only a small fraction of the history of climate variations. The short time period of the observed Arctic temperature change are not sufficient to represent the full range of its natural variability and to fully assess feedbacks about air-sea interactions, climate,



and ecosystems, it is still necessary to study the long-term changes, especially the millennium-scale changes, which can help shed more light on Arctic climate change in the future. For the past two millennia, temperature reconstructions (such as tree-ring, sediment and ice core records) from PAGES2k, and model data show a millennial cooling trend in the late Holocene, particularly in the Atlantic Arctic compared to the Pacific Arctic (Zhong et al., 2018). Zhong et al. (2018) presents that this cooling pattern was caused by both a weaker North Atlantic subpolar gyre and a stronger Aleutian low. The Holocene (past 11,700 years) shows millennial scale climate variations forced by changes in insolation due to orbital changes. The early-mid Holocene period is known as the Holocene thermal maximum (HTM) due to an average 5% increase in solar radiation compared to the present (Berger, 1978). The warm climate conditions were particularly pronounced at high latitudes in the early-to-mid Holocene, which is usually associated with the insolation forcing (Kaufman et al., 2004; Larsen et al., 2015; Gajewski, 2015; Briner et al., 2016; Renssen et al., 2012). Previous work examining the response to Arctic temperature change has either focused only on the trend over the whole Arctic and neglected potential regional asymmetry, or used only reconstruction data. The asymmetry of temperature change in the Arctic throughout the Holocene period, however, is evident (Fig. 1), likely associated with responses of climate modes to external climate forcings. The uncertainty and the low spatial coverage of reconstruction in temperature changes from proxy data makes it difficult to fully understand the Arctic temperature changes during the Holocene.

To overcome these limitations, in this study a state-of-the-art climate model, the Community Earth System Model (CESM), and a recent compilation of temperature proxy data are used to investigate the characteristics of the regional temperature changes in the Arctic. Through the analysis of changes in sea ice, sea level pressure, and orbital forcing, the governing factors that drive the asymmetric temperature variability are also identified, which is essential for future investigation of high-latitude temperature changes impact on the climate. The structure of this article is as follows. Sect. 2 describes the proxy and model data used in the current study. In Sect. 3, we summarized the temperature asymmetric changes reflected in the proxy and model data in the high latitudes of the Northern Hemisphere, while the changes in sea ice and sea level pressure during the Holocene are presented in Sect. 4. Finally, a summary and discussion are given in Sect. 5.

90 **2 Method and data**

2.1 The CESM Model and the transient simulations

This study analyzes a new transient simulation result based on the CESM, named NNU-Hol (Nanjing Normal University-Holocene), which considers more comprehensive external forcings for the Holocene climate change. The CESM is a fully-coupled, global climate model, which was launched by the National Center for Atmospheric Research (NCAR) in June 2010. It is an Earth System Model developed on the basis of CCSM. The CESM includes components for atmosphere, ocean, sea ice, as well as the land surface, and considers atmospheric chemistry, biogeochemistry, and anthropogenic forcing. It is widely used to study the mechanism of the changes in climate and environment, the interaction between natural and anthropogenic forcing for climate and for scenarios of future climate change (Wang et al., 2008; Zheng et al., 2008; Wang et al., 2016, 2018).



The CESM is coupled with several advanced modules, including the CAM5 (Community Atmosphere Model 5) used by the
100 atmosphere module, the POP2 (Parallel Ocean Program 2) used by the ocean module, the CLM4 (Community Land Model 4)
used by the land module, the CICE (The Los Alamos National Laboratory Sea-ice Model) used by the sea ice module and the
CISM2.0 (The Glimmer Ice Sheet Model 2.0) used by the land ice module. For a more detailed introduction, please visit the
official website of CESM (http://www.cesm.ucar.edu/models/cesm1.0-/notable_improvements.html).

In NNU-Hol, the CESM 1.0.3 was configured to simulate the transient climate evolution of the Holocene period at a horizontal
105 resolution of $3.75^{\circ} \times 3.75^{\circ}$, forced by several external forcings (orbital parameters, solar irradiance, volcanic eruptions,
greenhouse gases, and land use/land cover) accelerated by a factor of 10. With this acceleration method (Lorenz and Lohmann,
2004), climate trends and feedbacks from the past 11.95 ka BP to 1990 AD, imposed by the external forcing driven changes,
are represented in the experiments with 1199 model years to save computation resources. The solar irradiance forcing comes
from the reconstruction of (Vieira et al., 2011), and volcanic eruption comes from the ice core based reconstructions of (Gao
110 et al., 2021) and (Sigl et al., 2015). The greenhouse gas forcing data uses the reconstruction based on ice cores in (Joos and
Spahni, 2008). The data of land use/extra-land cover forcing comes from the HYDE 3.2.1 (the History Database of the Global
Environment, referred to as HYDE version 3.2.1) (Goldewijk et al., 2017) data set. The orbital parameters come from Berger
(1978). Wan et al. (2020) found that the global annual average temperature in the NNU-Hol All forcing simulation and
reconstruction records from Marcott et al. (2013) has similar trends and strengths, decreasing about 0.5 K during 5.0 to 0.15
115 ka BP. We explore the characteristics of changes in Arctic temperature during the Holocene and try to understand its underlying
mechanism based on the All forcing (AF) and orbital forcing (ORB) simulations in NNU-Hol.

There are, to our knowledge, 5 sets of climate simulations published so far covering the entire Holocene period, namely ECBilt-
CLIO (Timm and Timmermann, 2007), FOAM (Kutzbach et al., 2008), TraCE-21ka (Liu et al., 2009), FAMOUS (Smith and
Gregory, 2012) and LOVECLIM (Timmermann et al., 2014). The external forcings considered in these simulations are
120 generally a part of the combination of the Orbital Forcing (ORB), the Greenhouse Gases (GHG), the continental ice sheets
(ICE) and the Meltwater Flux (MWF). Except for TraCE-21ka, these simulations are accelerated by different factors.

2.2 Reconstructing Paleo Proxies data

In order to better understand the Holocene evolution of the earth system, a comprehensive database of paleoclimate records
was compiled by (Kaufman et al., 2020), which is named the Temperature 12k database.
125 Temperature 12k database is a global compilation of good-quality, published, temperature-sensitive proxy records (such as
lake sediment, marine sediment, peat, glacier ice and pollen, etc) through the entire Holocene period. The data is mainly
collected from previously published research, containing 1319 records (1162 from the Northern Hemisphere and 157 from the
Southern Hemisphere), distributed in 679 sites (including 470 terrestrial and 209 marine sites) where time period cover at least
4000 years. For our study we only selected records with a resolution finer than 400 years, 15% of these records have a resolution
130 of 50 years or finer, 39% have a resolution of 51 to 150 years, and 21% have a resolution of more than 250 years.



The data is mainly based on a collection of published reconstructions of Holocene temperature especially in the Northern Hemisphere (Routson et al., 2019; Marcott et al., 2013; Sundqvist et al., 2014; Chen et al., 2008; Wanner et al., 2011). Part of the data collected the global paleotemperature records from PAGES 2k Consortium 9 database. The compilation of Marsicek et al. (2018) provides most pollen-based paleotemperature records and the other part comes from public repositories (such as PANGAEA and World Data Service for Paleoclimatology, NOAA). The paleotemperature records in 209 marine sites are mainly from the US-based Data Assimilation for Deep Time (DADT) project and the compilations of the German Climate Modeling Initiative (PalMod) (Jonkers et al., 2020). More detailed information can be found at www.ncdc.noaa.gov/paleo/study/2733.

In order to investigate the changes in temperature over the Arctic area during the Holocene, we selected records from the site, which are located above 60 degrees north latitude, and eliminated some records with shorter time series (missing more than 2500 years during the Holocene), which leaves us with 52 records.

3 Result

3.1 Arctic Temperature Change

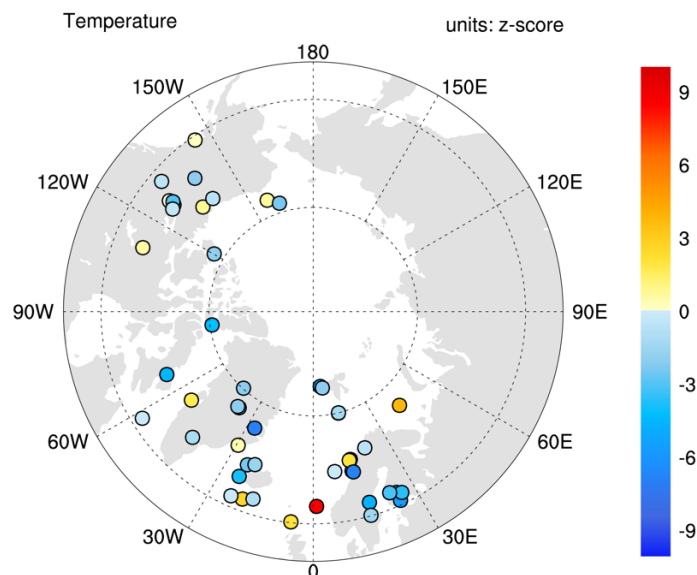
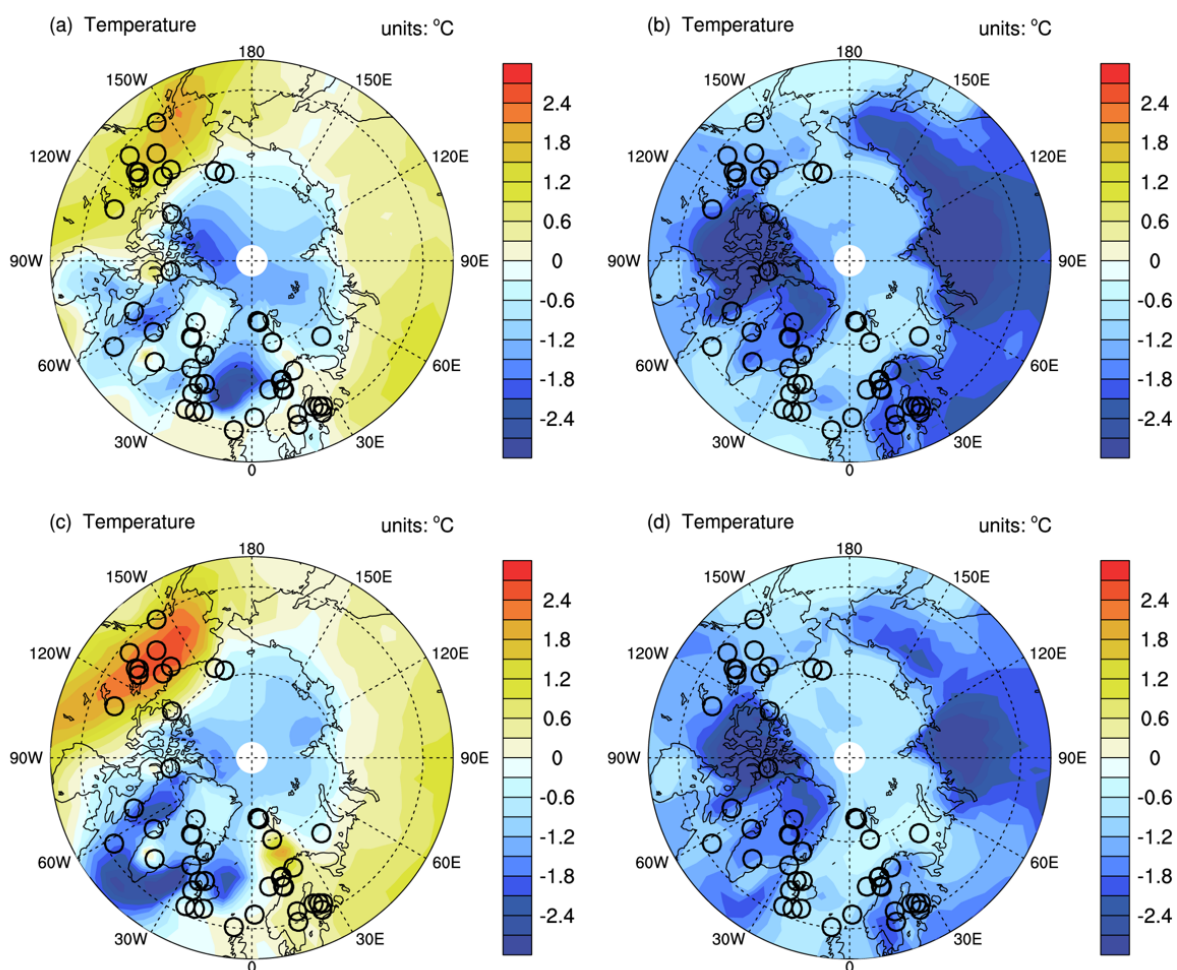


Figure 1: The annual temperature changes between two period (0-2 ka BP and 5-8 ka BP) in Reconstructions (Temperature 12k)

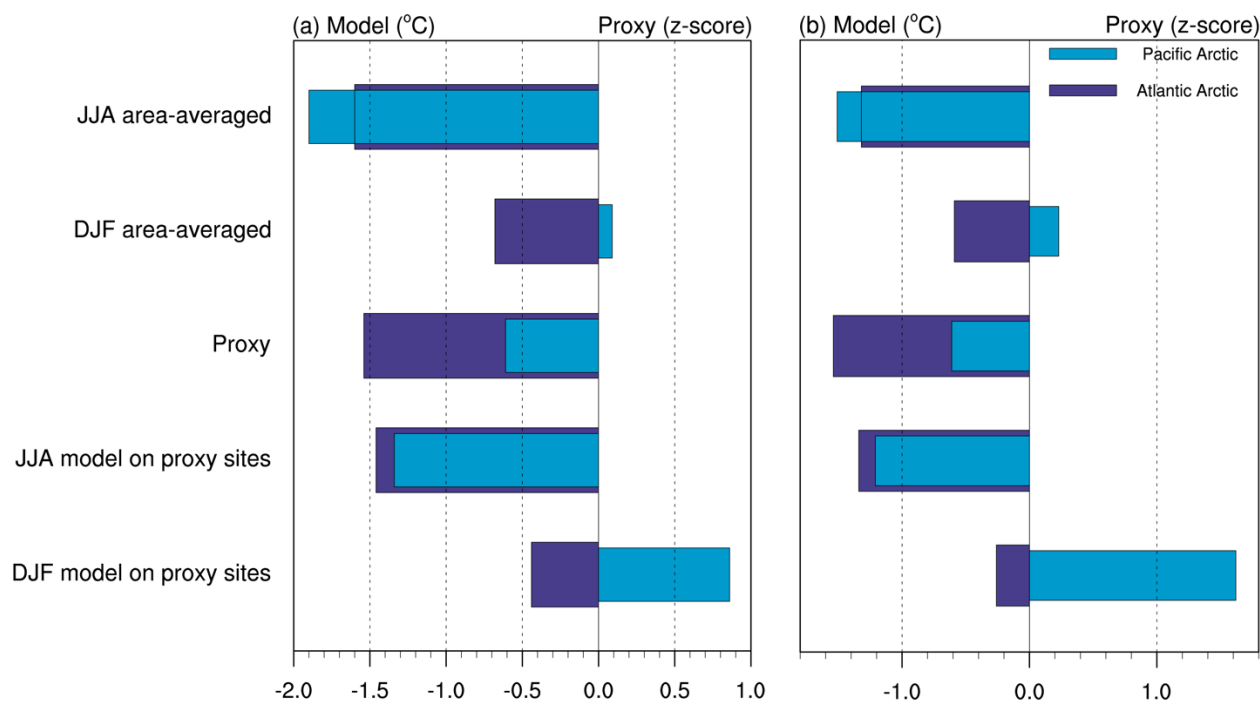
In order to demonstrate asymmetric temperature changes in the Arctic during the Holocene, we analyzed the two periods (0-2 ka BP and 5-8 ka BP) with the greatest temperature differences, based on the Temperature 12k database (Kaufman et al., 2020). The results are shown in Fig. 1, where the circles represent the site locations of the 52 selected records, with red indicating an increase in temperature between the late and the early-mid Holocene (0-2 ka BP and 5-8 ka BP), while the blue indicating and decreasing. The proxy records are mainly concentrated on the Atlantic coast, Europe, Greenland, and northern Canada. The



average temperature across the Arctic showed a cooling trend during the Holocene, which is consistent with previous findings (Marcott et al., 2013; Kaufman et al., 2004). To study the asymmetric changes in temperature, we divided the Arctic region into two parts, the Pacific Arctic (Lat > 60°N, Lon 90°W ~ 59°E) and the Atlantic Arctic (Lat > 60°N, Lon 60°E ~ 91°W). The proxy data shows that there is an asymmetric cooling between the two regions, with an average cooling of -1.54 °C in the Atlantic Arctic and -0.61 °C in the Pacific Arctic respectively. To further study the robustness of this asymmetric change in temperature, we likewise analyze it with model data, allowing us to also investigate the seasonal changes.



160 **Figure 2: (a) The DJF temperature changes between two period (0-2 ka BP and 5-8 ka BP) in NNU-Holocene All forcing simulations (Pacific Arctic:-0.44, Atlantic Arctic:1.00); (b) Same as (a) but for JJA (Pacific Arctic:3.98, Atlantic Arctic:3.81) (c) The DJF temperature changes between two period (0-2 ka BP and 5-8 ka BP) in NNU-Holocene ORB forcing simulations (Pacific Arctic:-0.80, Atlantic Arctic:1.75); (d) Same as (c) but for JJA (Pacific Arctic:7.48, Atlantic Arctic:6.07)**

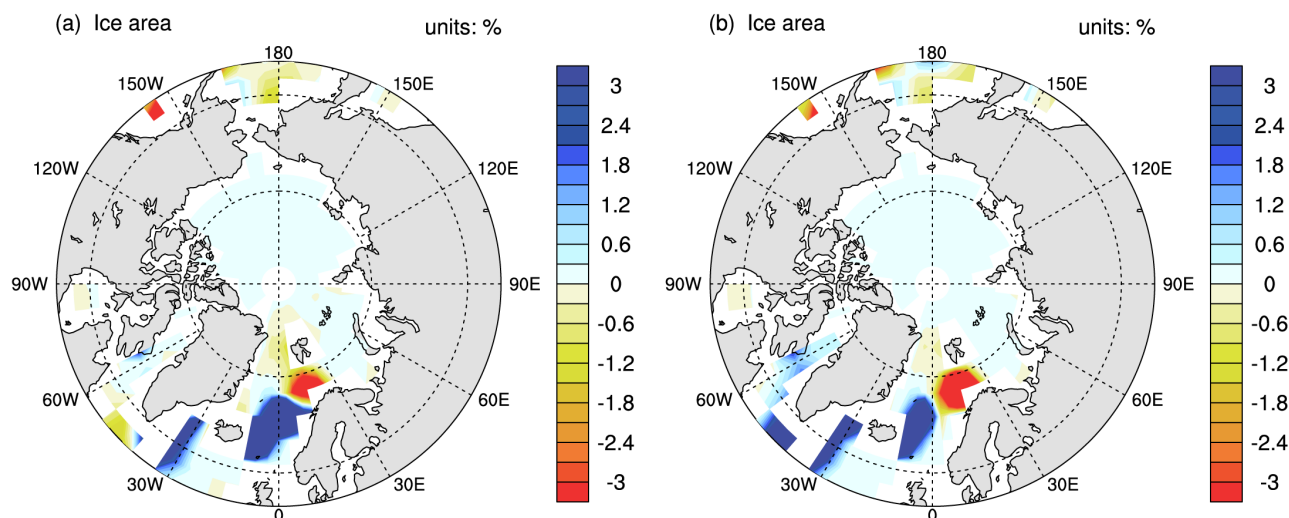


165 **Fig.3 1) Model area average temperature change in JJA; 2) Model area average temperature change in DJF; 3) Annual temperature change in Proxy; 4) Model JJA average temperature change on proxy sites; 5) Model DJF average temperature change on proxy sites (a: AF simulation, b: ORB simulation);**

Here we use the model data based on the CESM, the “NNU-Hol”, and we choose data from All Forcing simulation (AF) and Orbital forcing simulation (ORB) in order to assess the most realistic temperature changes (AF) and the role of the orbital forcing (ORB) in the changes during the Holocene. As shown in Figure 2, to better understand the asymmetry, we further
 170 analyze the temperature changes in two seasons, DJF (December, January and February) and JJA (June, July and August). The results from AF and ORB show a similar pattern. In the JJA, the Arctic exhibits a comparable cooling trend in the Atlantic sector and the North Pacific sector, with cooling centers in Eurasia and northeastern America. However, there is significant regional asymmetric cooling in the DJF (-0.67 for Atlantic Arctic average cooling and 0.09 for Pacific Arctic average warming in AF), with the Arctic Ocean, the North Atlantic Ocean and Greenland are cooling, while the land and North Pacific Ocean
 175 are warming. Northern Canada, where numerous proxy sites are located, is the center of the temperature warming, with the cooling center changing from the Straits in the AF to the North Atlantic in the ORB. We can see more clearly the difference of temperature asymmetry in two seasons through Figure 3, and the intensity of the asymmetry is more pronounced at the proxy sites. In the DJF of AF, the average cooling is -0.44 for the Atlantic Arctic proxy site and the average warming is 0.85 for the Pacific Arctic proxy site, while in the ORB it is -0.25 and 1.61, respectively. Fig.3 shows that the temperature difference
 180 between the Pacific and Atlantic Arctic is neglectable for either the regional average or the sites station average in JJA. Therefore, the asymmetric temperature changes of the Atlantic and Pacific Arctic is dominated by the changes in DJF.

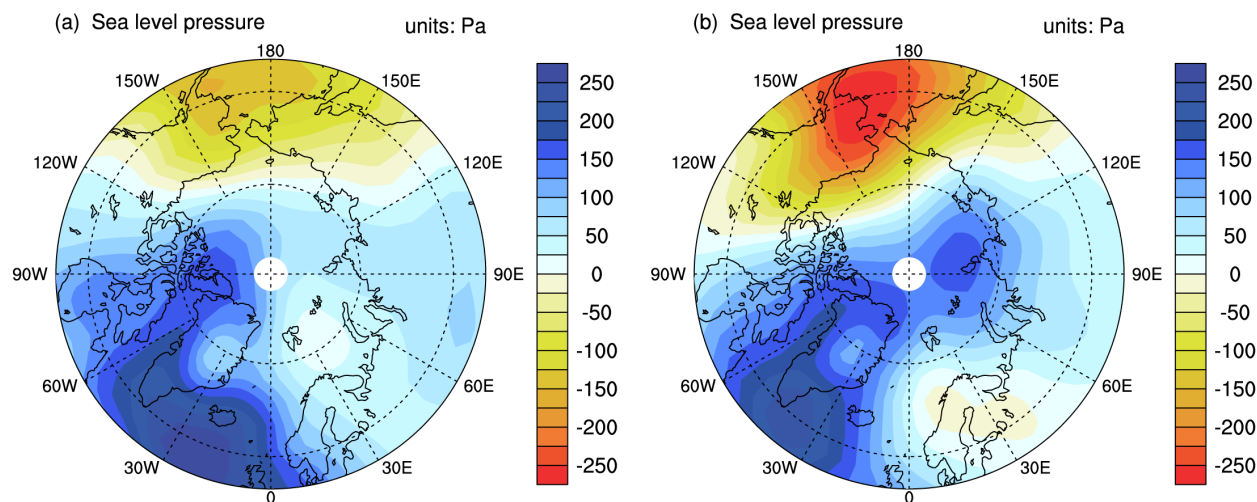


3.2 Sea Ice Change (Aice, March) and SLP Change



185 **Fig.4 (a) The March sea ice area (aice) changes between two period (0-2 ka BP and 5-8 ka BP) in NNU-Holocene All forcing simulation (regional average on Pacific Arctic:0.02% and Atlantic Arctic:0.29%); (b) Same as (a) but for ORB forcing simulation (regional average on Pacific Arctic:0.04%, Atlantic Arctic:0.29%);**

The past research has shown that sea ice is always an important factor when we discuss Arctic climate change (Jenkins and Dai, 2021). Arctic temperature changes are often tightly linked to sea ice changes, with temperature causing changes in the expansion of sea ice cover and therefore changes in surface albedo, further amplifying climate change at Arctic region
190 (Wohlfahrt et al., 2004; Renssen, H. et al., 2005; Braconnot et al., 2007). The simulations show that the temperature asymmetry is closely related to the asymmetric change in sea-ice pattern. The difference in March sea ice area between the two periods (0-2 ka BP and 5-8 ka BP) is fairly consistent in the AF and ORB simulations. During the Holocene, sea ice increased throughout the Arctic, especially around the Norwegian Sea and Davis Strait, with the exception of the Fram Strait and the Barents Sea, where sea ice area declined significantly. The large expansion of sea ice in the North Atlantic and the slight
195 decrease in sea ice in the North Pacific leads to strong differences in surface albedo between the two regions, with more reflection of radiation in the North Atlantic and more absorption in the North Pacific. In addition, greater heat storage in subsurface ocean in the North Pacific were discharged in winter (Dai, 2021) compared to the North Atlantic, which contributes to the stronger asymmetry during winter (Fig. 3).

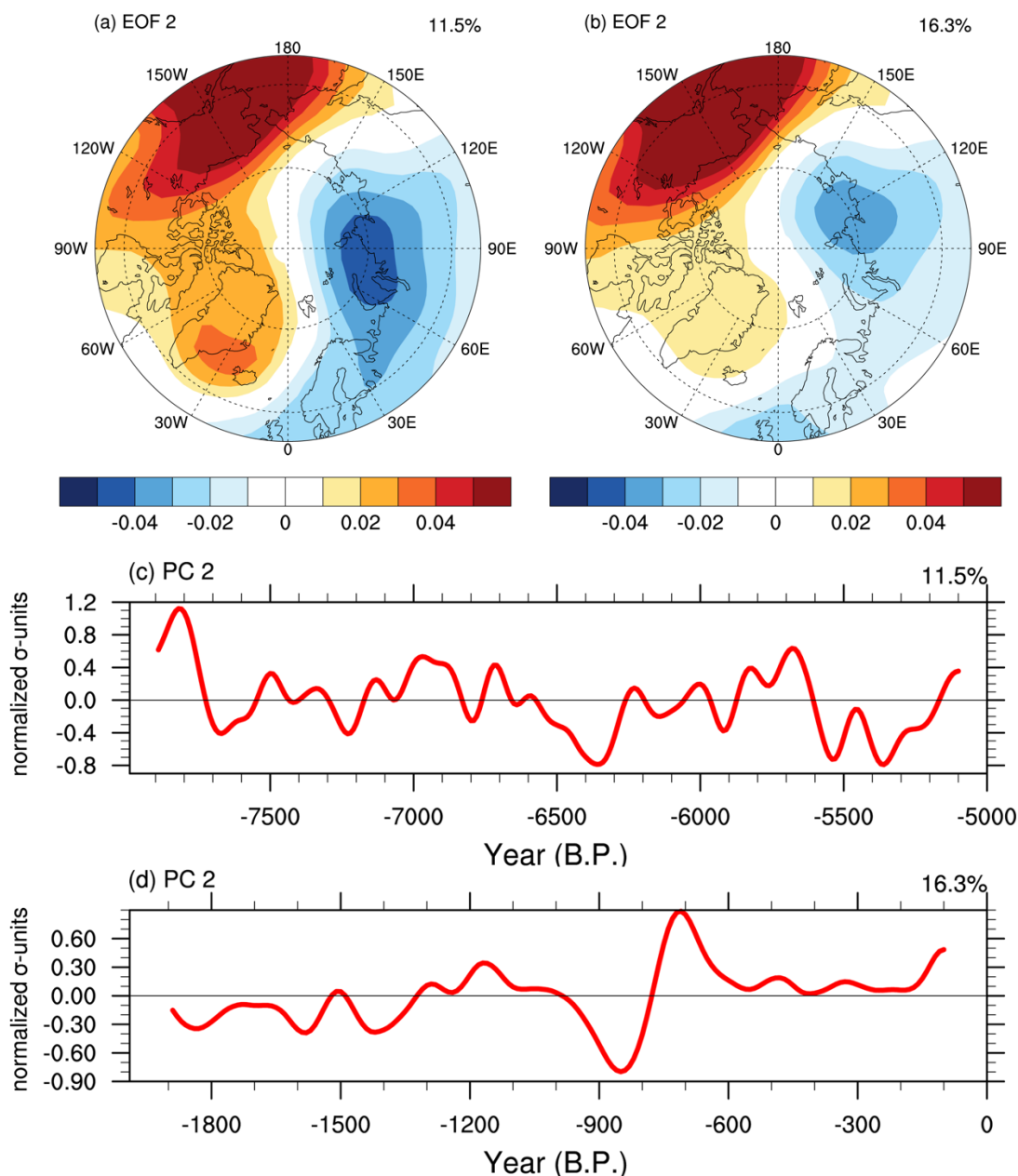


200 **Fig.5 (a) The DJF sea level pressure changes between two period (0-2 ka BP and 5-8 ka BP) in NNU-Holocene All forcing simulation;**
205 **(b) Same as (a) but for ORB forcing simulation;**

To understand the dynamical aspects of the stronger cooling in the North Atlantic, we investigate the regional-scale atmospheric circulation and surface wind variations related to sea-ice transport. We focus our analysis on the December–February season, because these months yield the largest impact of temperature asymmetry. In DJF, the sea level pressure (SLP)
205 has a distinct dipole distribution. Sea level pressure increases in the North Atlantic and decreases in the North Pacific. The low pressure in the North Pacific is intensifying during the late Holocene. Many studies (Wu et al., 2006; Niebauer et al., 1999; Stabeno et al., 2001; Rodionov et al., 2005) have demonstrated that the stronger low pressure transported warm air from the south to the North Pacific, resulting in higher temperatures in the North Pacific, offsetting parts of the Holocene cooling trend in the North Pacific and causing sea ice expansion in the North Atlantic due to atmospheric circulation. We hypothesize that
210 this contributes to the regional asymmetry in Arctic temperatures. The results of the ORB simulations are more significant than those of the AF, indicating that the orbital forcing plays the most important role in generating this asymmetry.



3.3 EOF of SLP and UV wind regression

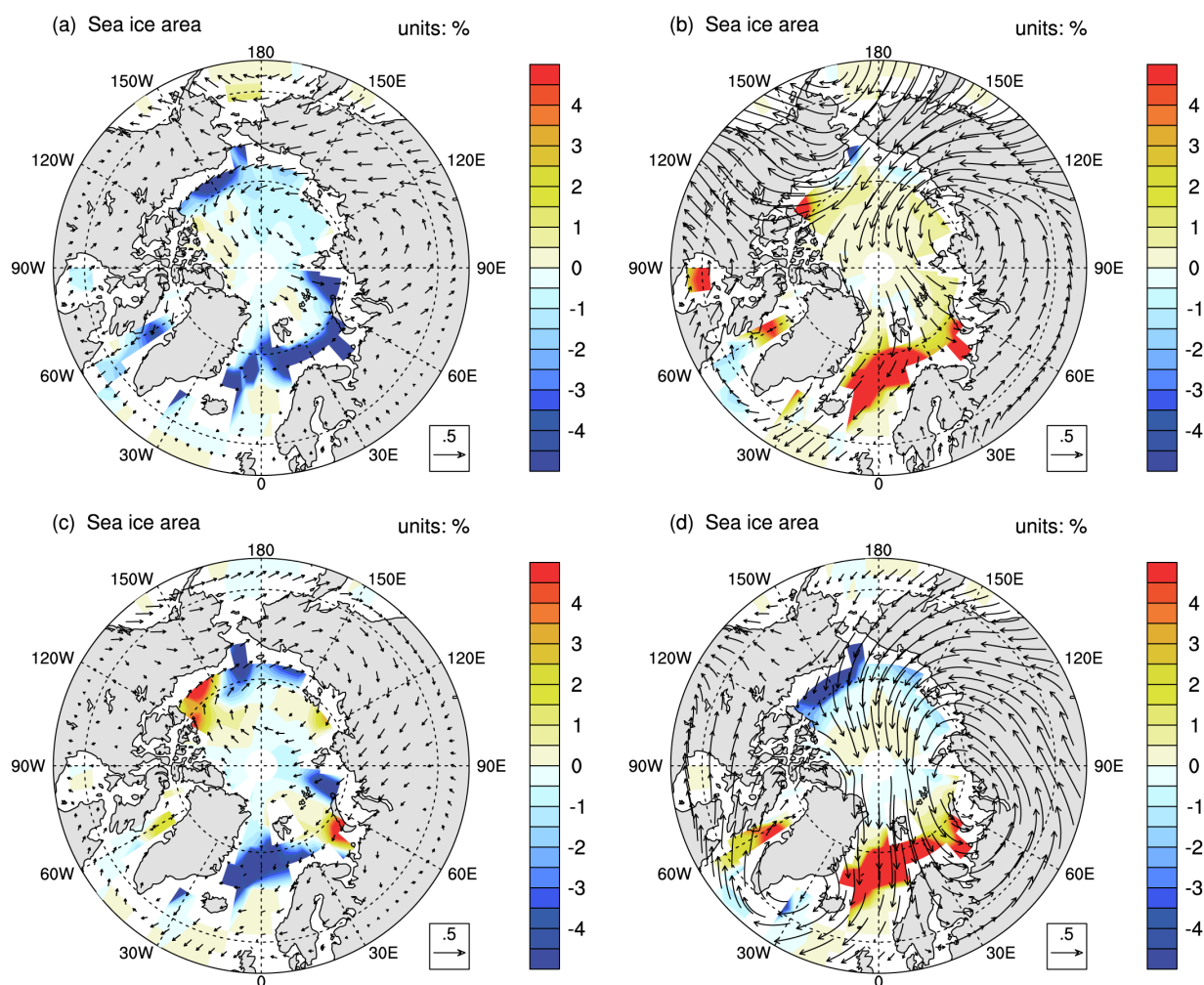


215 **Fig.6** The second EOF (EOF2) pattern of the Sea level pressure in NNU-Holocene All forcing simulations during 5-8 ka BP (a) and 0-2 ka BP (b); The second Principal Component (PC2) time series of the Sea level pressure changes in NNU-Holocene All forcing simulations during 5-8 ka BP (c) and 0-2 ka BP (d);

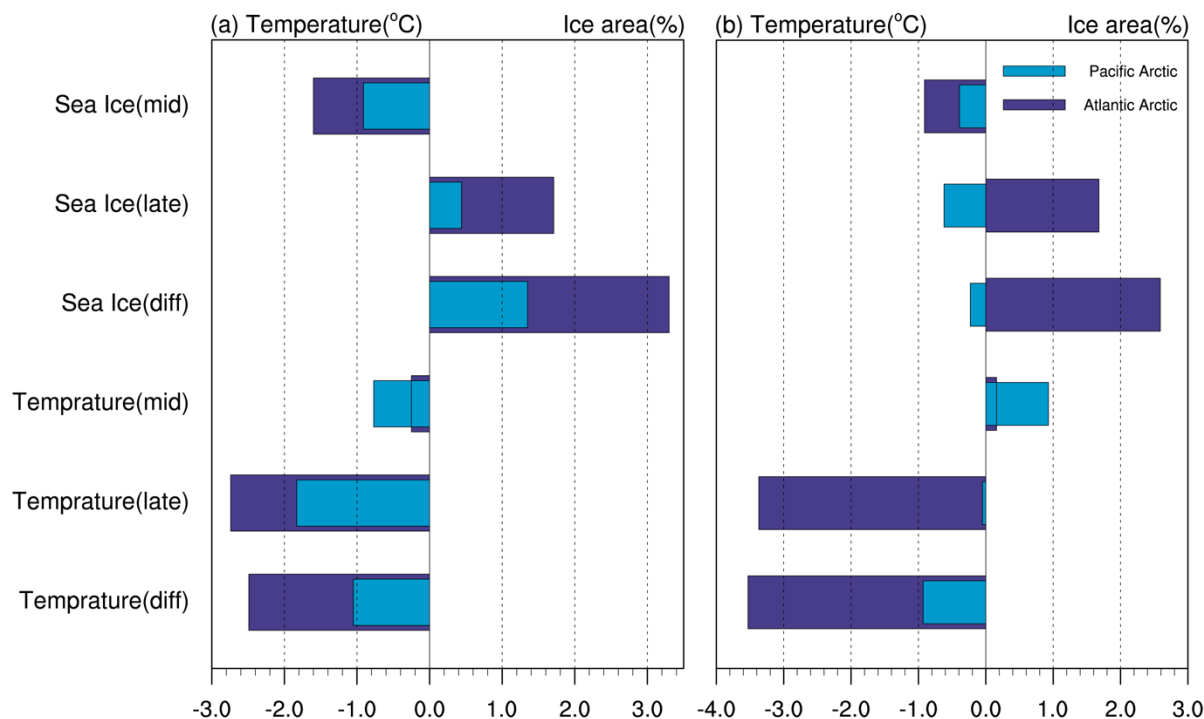
Previous studies have established that atmospheric circulation anomalies in the Arctic atmosphere, dipole structure anomalies, are closely related to sea ice (Wu et al., 2006; Watanabe et al., 2006; Choi et al., 2019). The Arctic dipole strongly influences



220 sea ice movement and sea ice export. The dipole anomaly corresponds to the second leading mode of the EOF of the monthly
mean sea level pressure (SLP) north of 60 degrees north latitude in winter. To corroborate our hypothesis, we analyze the
Arctic dipole and the results are shown in Figure 6. In the AF simulation, the EOF pattern of the SLP is similar for both periods
(0-2 ka BP and 5-8 ka BP), with the second mode shows an Arctic dipolar distribution with the center of variability located in
the North Pacific and in northern Eurasia, accounting for 11.5% (5-8 ka BP) and 16.3% (0-2 ka BP) of the variance. The
225 difference in SLP between the two periods does show a similar dipole pattern, but combined with the stronger SLP in the late
Holocene than in the early-mid Holocene shown above, it can be assumed that the stronger Arctic dipole in the late period had
a greater role in influencing sea ice. Therefore, the intensity of the dipole mode appears to dominate the sea-ice distribution in
the Arctic, and the hypothesis can be verified.



230 Fig.7 The regression of UV wind and sea ice based on the PC2 of the Sea level pressure in NNU-Holocene AF simulation during 5-8
ka BP (a) and 0-2 ka BP (b); in the NNU-Holocene ORB simulation during 5-8 ka BP (c) and 0-2 ka BP (d);



235 **Fig.8 1) Average change in the regression of Sea ice on the PC2 of the SLP in early-mid Holocene; 2) same as 1) in late Holocene; 3) Differences in the regressions of Sea ice on PC2 of SLP between two period; 4) The regression of temperature average change in early-mid Holocene; 5) same as 4) in late Holocene; 6) Differences in the regressions of temperature on PC2 of SLP between two period (a: AF simulation, b: ORB simulation);**

We compare the two spatial patterns of the sea ice and UV wind field regression onto PC2 (Fig. 7). In the late Holocene, the Bering Strait and East Siberia were influenced by warm winds from the south, increasing the temperature in these areas. On the other hand, the winds cause the Arctic Ocean sea ice to expand to the North Atlantic Ocean through Fram Strait transfer. This leads to more sea ice in the Atlantic Ocean, and in turn, more radiant heat reflected and surface cooling, forming a positive sea ice feedback. This wind pattern contributes to the asymmetry of temperature variations between the North Atlantic and the North Pacific. In the late Holocene, the wind field characteristics are more pronounced than those in the early-mid Holocene, and thus the temperature asymmetry is more significant. As shown in Fig. 8, the regression of sea ice on the PC2 of SLP increased by 1.71% in North Atlantic and 0.44% in North Pacific during the late Holocene, while decreased by -1.60% and -0.91% during the early-mid Holocene. The corresponding asymmetric cooling in the early-mid to late Holocene was -2.74°C in the North Atlantic and -1.83°C in the North Pacific. The results of the ORB simulations in terms of the asymmetry are similar to the AF simulations, but stronger. The regression of temperature shows a cooling of -3.37°C and -0.05°C in the North Atlantic and North Pacific, respectively, during the late Holocene. A centre of the Arctic dipole is closer to Greenland during the late Holocene. Stronger, warmer southerly winds in the late Holocene raises temperatures in the Pacific Arctic leading to more pronounced asymmetric temperature changes in the Arctic in ORB.

240
245



250 3.4 The connection between Arctic Dipole pattern and PDO

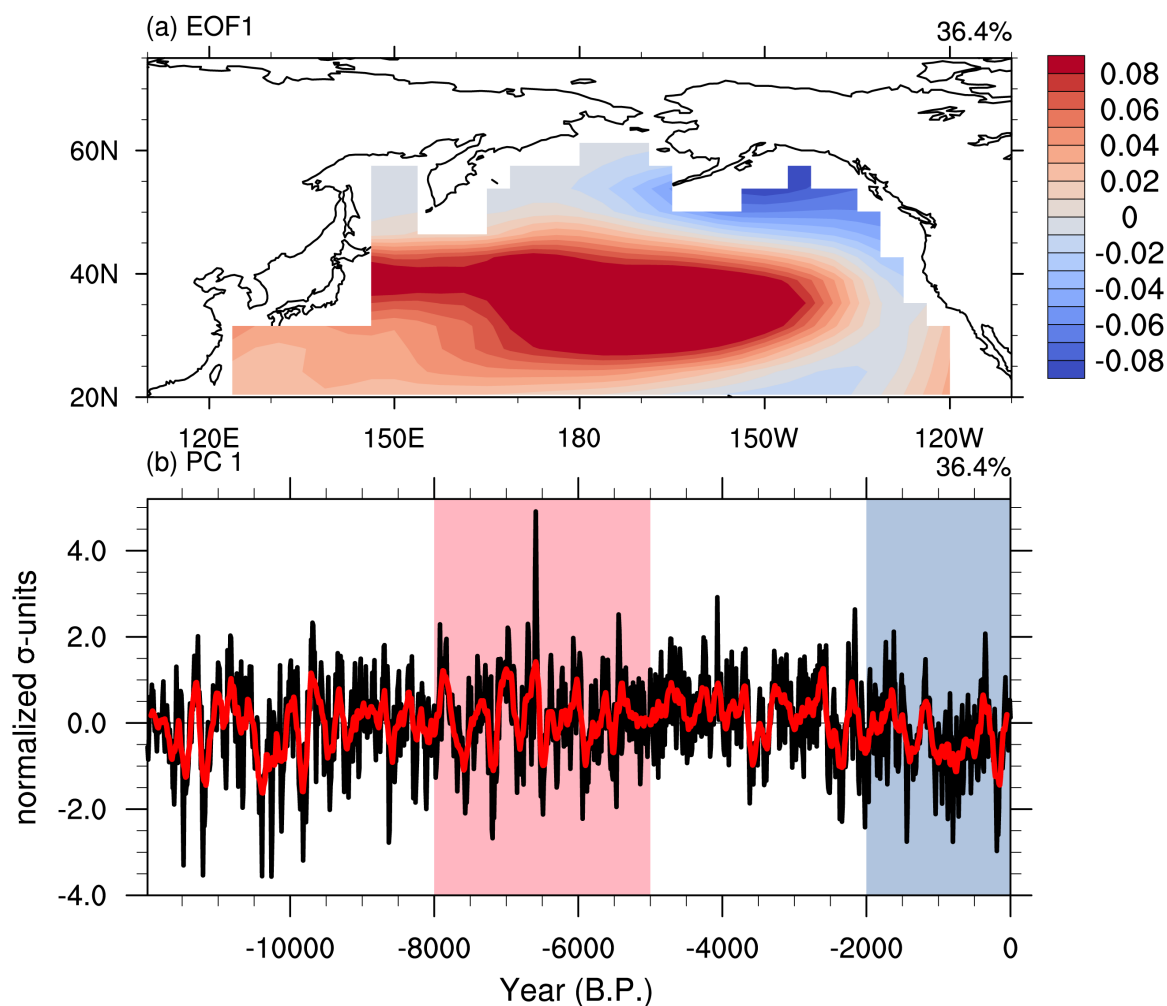
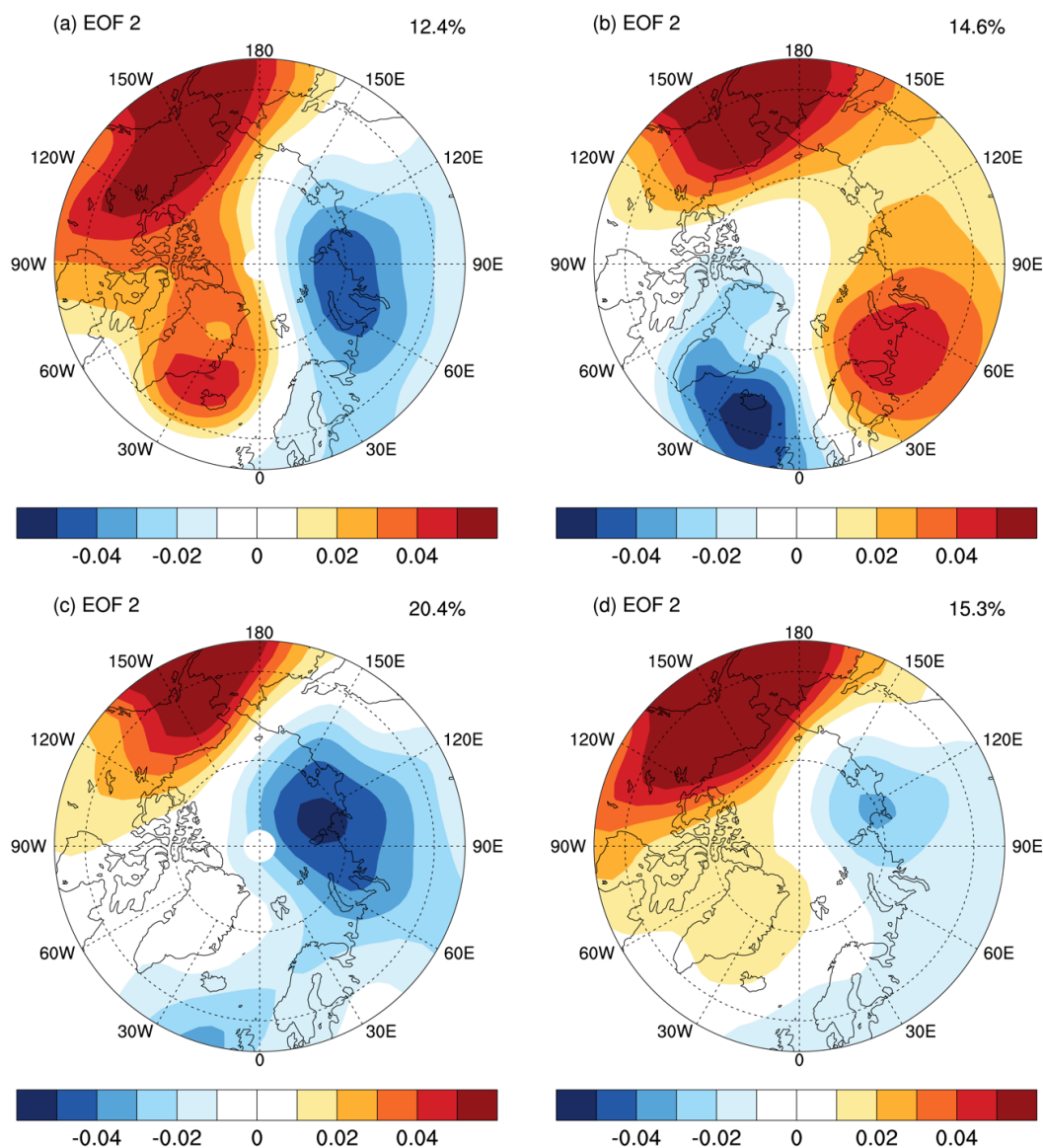


Fig.9 (a) The leading pattern (EOF1) of sea surface temperature (SST) anomalies in the North Pacific basin (poleward of 20°N); (b) The Holocene PDO index is defined by the leading Principal Component (PC1) time series of EOF1;



255 **Fig.10 (a) The leading pattern (EOF1) of sea level pressure (SLP) in positive PDO years during the early-mid Holocene; (b) same as (a) in negative PDO years during the early-mid Holocene; (c) same as (a) in positive PDO years during the late Holocene; (d) same as (a) in negative PDO years during the late Holocene;**

Previous studies (Choi et al., 2019) have shown that the different phases of PDO are related to the Arctic Dipole mode. Figure 9 shows the changes in the PDO index, which is defined by the leading principal component (PC1) time series of the sea surface temperature (SST) anomaly in North Pacific during the Holocene. The index indicates that negative PDO dominates the late Holocene, while the positive and negative PDO phases oscillate during the early-mid Holocene. We separate the positive phase and negative phase PDO years, and perform EOF analysis on the composites of PDO two phases years to investigate if trends in the PDO can explain changes in the Arctic Dipole pattern (Fig. 10). The results show that the EOF



pattern of SLP mainly depends on the Arctic dipole in the negative PDO year in the late Holocene with the spatial correlation
265 coefficient 0.99 (compare with Fig. 6b). In the early-mid Holocene, negative PDO year accounted for 38% and positive PDO
year accounted for 62%. Therefore, The EOF pattern of the SLP in positive PDO years became dominant during the early-mid
Holocene, with the spatial correlation coefficient is 0.96 (compare Fig. 6a). Therefore, we propose that orbital forcing affects
the changes of the Arctic dipole by regulating PDO, and further causes the appearance of temperature asymmetry in the Arctic
region. However, it should be pointed out that although the PDO is closely related to the Arctic dipole and the orbital forcing
270 in earlier research (Choi et al., 2019; Kirby et al., 2010; Barron and Anderson, 2011), only the relationship between PDO and
the Arctic dipole is reflected in our study. The orbital forcing mechanism of PDO specifically for our simulations are not fully
explored as it is beyond the scope of this study.

4 Discussion

The results indicate that the sea level pressure and sea ice changes are responsible for the asymmetric Arctic cooling, since
275 these two factors show similar asymmetric variations over the North Atlantic and the North Pacific. Compared with the early-
mid Holocene, the sea ice expanded in the North Atlantic during the late Holocene, which leads to more cooling in the Atlantic
Arctic due to its feedback. On the other hand, the Arctic dipole pattern, which plays an important role in sea-ice expansion in
the North Atlantic, promotes more cooling in Atlantic Arctic and raising the temperature in the Pacific Arctic with warm
southerly winds, exacerbating the temperature asymmetry. The asymmetric pattern is consistent with the asymmetric cooling
280 in the Arctic over the past 2,000 years (Zhong et al., 2018). Our results are in line with the hypothesis that sea level pressure
and sea ice play the important role in asymmetric cooling.

Earlier work was more focused on the effects of the Arctic amplification in recent decades. Based on the observation data, it
is assumed that AA will further increase the possibility of extreme weather in mid-latitude regions by increasing the
temperature gradient from the equator to the pole in dynamic ways. However, the mechanism behind this is still not fully
285 understood (Xue et al., 2017; Cohen et al., 2018; Chen et al., 2015; Vavrus, 2018; Screen, 2017). For long-term Arctic climate
research, it is mainly the study of temperature trend changes based on reconstructed proxy data (Kaufman et al., 2004; Meyer
et al., 2015; Briner et al., 2016). This study provides a new insight into the regional characteristics of Arctic temperature
changes. With the addition of our model analysis this study improves our understanding of the drivers of variability changes
in Arctic temperature on centennial and millennial time scales. The role of sea ice and sea level pressure offers an explanation
290 for the regional differences in Arctic temperature trends. These results can have useful implications on predicting the climate
changes at mid-latitudes in the global warming background.

The study demonstrates that the asymmetry of the orbital forcing-only simulations is greater than that of the full forcing
simulation. Stronger response to orbital forcing implies that the other forcings (e.g. GHG) may compensate this asymmetry.
Nevertheless, the individual contribution of each forcing has not been clearly investigated in our study. In particular, the GHG
295 forcing, which is the most crucial driver in the near-future climate compared to orbital forcing, has not changed significantly



during the Holocene. To fully understand the potential compensation effects induced by GHG, the next steps regarding paleo Arctic temperature studies are compiling more high-resolution, seasonal paleoclimate temperature data, employing a full set of single forcing simulations (e.g. TraCE-21ka, Liu et al., 2014), and analyzing and comparing the results of multiple models for reducing the uncertainty of the models and the validation of the roles of different forcing.

300 5 Summary

The findings from this paper suggests that the Arctic temperature has an asymmetric cooling trend with more cooling over the Atlantic Arctic (-1.54 °C) than the Pacific Arctic (-0.61 °C) during the Holocene, based on Temperature 12k database (Kaufman et al., 2020). In our modeling results, a similar asymmetric change of temperature in the Arctic can be reproduced by CESM, dominated by orbital forcing. Our model simulations show the strongest cooling in the Arctic Ocean, Greenland Island, and the North Atlantic, while the temperature in northern Eurasia and northern Canada shows a warming trend. There is a seasonal difference in the asymmetric cooling trend, which is dominated by the DJF temperature variability. The Arctic dipole mode of sea level pressure and sea ice play a major role in asymmetric temperature changes, which is possibly modulated by orbital forcing of PDO.

Acknowledgments

310 This work was jointly supported by the National Natural Science Foundation of China (Grant Nos. 42130604, 42105044, 41971108, and 42111530182) and the Priority Academic Program Development of Jiangsu Higher Education Institutions (Grant No. 164320H116). J. Sjolte was supported by the strategic research program of ModELing the Regional and Global Earth system (MERGE) hosted by the Faculty of Science at Lund University. Z. Lu received funding from FORMAS mobility (Grant no. 2020-02267)

315 References

- Aagaard, K. and Carmack, E. C.: The role of sea ice and other fresh water in the Arctic circulation, 94, 14485–14498, <https://doi.org/10.1029/JC094iC10p14485>, 1989.
- Alekseev, G. V., Johannessen, O. M., Korablev, A. A., Ivanov, V. V., and Kovalevsky, D. V.: Interannual variability in water masses in the Greenland Sea and adjacent areas, 20, 201–208, <https://doi.org/10.1111/j.1751-8369.2001.tb00057.x>, 2001.
- 320 Barnes, E. A. and Screen, J. A.: The impact of Arctic warming on the midlatitude jet-stream: Can it? Has it? Will it?, 6, 277–286, <https://doi.org/10.1002/wcc.337>, 2015.
- Barron, J. A. and Anderson, L.: Enhanced Late Holocene ENSO/PDO expression along the margins of the eastern North Pacific, *Quaternary International*, 235, 3–12, <https://doi.org/10.1016/j.quaint.2010.02.026>, 2011.



- Berger, A.: Long-Term Variations of Daily Insolation and Quaternary Climatic Changes, 35, 2362–2367,
325 [https://doi.org/10.1175/1520-0469\(1978\)035<2362:LTVODI>2.0.CO;2](https://doi.org/10.1175/1520-0469(1978)035<2362:LTVODI>2.0.CO;2), 1978.
- Blackport, R. and Kushner, P. J.: The Role of Extratropical Ocean Warming in the Coupled Climate Response to Arctic Sea
Ice Loss, 31, 9193–9206, <https://doi.org/10.1175/JCLI-D-18-0192.1>, 2018.
- Braconnot, P., Otto-Bliessner, B., Harrison, S., Joussaume, S., Peterchmitt, J.-Y., Abe-Ouchi, A., Crucifix, M., Driesschaert,
E., Fichefet, T., Hewitt, C. D., Kageyama, M., Kitoh, A., Loutre, M.-F., Marti, O., Merkel, U., Ramstein, G., Valdes, P., Weber,
330 L., Yu, Y., and Zhao, Y.: Results of PMIP2 coupled simulations of the Mid-Holocene and Last Glacial Maximum –
Part 2: feedbacks with emphasis on the location of the ITCZ and mid- and high latitudes heat budget, 3, 279–296,
<https://doi.org/10.5194/cp-3-279-2007>, 2007.
- Briner, J. P., McKay, N. P., Axford, Y., Bennike, O., Bradley, R. S., de Vernal, A., Fisher, D., Francus, P., Fr chette, B.,
Gajewski, K., Jennings, A., Kaufman, D. S., Miller, G., Rouston, C., and Wagner, B.: Holocene climate change in Arctic
335 Canada and Greenland, *Quaternary Science Reviews*, 147, 340–364, <https://doi.org/10.1016/j.quascirev.2016.02.010>, 2016.
- Chen, F., Yu, Z., Yang, M., Ito, E., Wang, S., Madsen, D. B., Huang, X., Zhao, Y., Sato, T., John B. Birks, H., Boomer, I.,
Chen, J., An, C., and W nnemann, B.: Holocene moisture evolution in arid central Asia and its out-of-phase relationship with
Asian monsoon history, *Quaternary Science Reviews*, 27, 351–364, <https://doi.org/10.1016/j.quascirev.2007.10.017>, 2008.
- Chen, G., Lu, J., Burrows, D. A., and Leung, L. R.: Local finite-amplitude wave activity as an objective diagnostic of
340 midlatitude extreme weather, 42, 10,952-10,960, <https://doi.org/10.1002/2015GL066959>, 2015.
- Choi, N., Kim, K.-M., Lim, Y.-K., and Lee, M.-I.: Decadal changes in the leading patterns of sea level pressure in the Arctic
and their impacts on the sea ice variability in boreal summer, 13, 3007–3021, <https://doi.org/10.5194/tc-13-3007-2019>, 2019.
- Cohen, J.: An observational analysis: Tropical relative to Arctic influence on midlatitude weather in the era of Arctic
amplification, 43, 5287–5294, <https://doi.org/10.1002/2016GL069102>, 2016.
- 345 Cohen, J., Screen, J. A., Furtado, J. C., Barlow, M., Whittleston, D., Coumou, D., Francis, J., Dethloff, K., Entekhabi, D.,
Overland, J., and Jones, J.: Recent Arctic amplification and extreme mid-latitude weather, *Nature Geosci*, 7, 627–637,
<https://doi.org/10.1038/ngeo2234>, 2014.
- Cohen, J., Pfeiffer, K., and Francis, J. A.: Warm Arctic episodes linked with increased frequency of extreme winter weather
in the United States, *Nat Commun*, 9, 869, <https://doi.org/10.1038/s41467-018-02992-9>, 2018.
- 350 Dai, H.: Roles of Surface Albedo, Surface Temperature and Carbon Dioxide in the Seasonal Variation of Arctic Amplification,
48, e2020GL090301, <https://doi.org/10.1029/2020GL090301>, 2021.
- Delworth, T. L. and Knutson, T. R.: Simulation of Early 20th Century Global Warming, 287, 2246–2250,
<https://doi.org/10.1126/science.287.5461.2246>, 2000.
- Deser, C., Tomas, R. A., and Sun, L.: The Role of Ocean–Atmosphere Coupling in the Zonal-Mean Atmospheric Response to
355 Arctic Sea Ice Loss, 28, 2168–2186, <https://doi.org/10.1175/JCLI-D-14-00325.1>, 2015.
- Deser, C., Sun, L., Tomas, R. A., and Screen, J.: Does ocean coupling matter for the northern extratropical response to projected
Arctic sea ice loss?, 43, 2149–2157, <https://doi.org/10.1002/2016GL067792>, 2016.



- Francis, J. and Skific, N.: Evidence linking rapid Arctic warming to mid-latitude weather patterns, 373, 20140170, <https://doi.org/10.1098/rsta.2014.0170>, 2015.
- 360 Francis, J. A. and Hunter, E.: Drivers of declining sea ice in the Arctic winter: A tale of two seas, 34, <https://doi.org/10.1029/2007GL030995>, 2007.
- Francis, J. A. and Vavrus, S. J.: Evidence linking Arctic amplification to extreme weather in mid-latitudes, 39, <https://doi.org/10.1029/2012GL051000>, 2012.
- Francis, J. A. and Vavrus, S. J.: Evidence for a wavier jet stream in response to rapid Arctic warming, *Environ. Res. Lett.*, 10, 014005, <https://doi.org/10.1088/1748-9326/10/1/014005>, 2015.
- 365 Funder, S., Goosse, H., Jepsen, H., Kaas, E., Kjær, K. H., Korsgaard, N. J., Larsen, N. K., Linderson, H., Lyså, A., Möller, P., Olsen, J., and Willerslev, E.: A 10,000-Year Record of Arctic Ocean Sea-Ice Variability—View from the Beach, 333, 747–750, <https://doi.org/10.1126/science.1202760>, 2011.
- Gajewski, K.: Quantitative reconstruction of Holocene temperatures across the Canadian Arctic and Greenland, *Global and Planetary Change*, 128, 14–23, <https://doi.org/10.1016/j.gloplacha.2015.02.003>, 2015.
- 370 Gao, C., Ludlow, F., Matthews, J. A., Stine, A. R., Robock, A., Pan, Y., Breen, R., Nolan, B., and Sigl, M.: Volcanic climate impacts can act as ultimate and proximate causes of Chinese dynastic collapse, *Commun Earth Environ*, 2, 1–11, <https://doi.org/10.1038/s43247-021-00284-7>, 2021.
- Goosse, H. and Fichefet, T.: Importance of ice-ocean interactions for the global ocean circulation: A model study, 104, 23337–23355, <https://doi.org/10.1029/1999JC900215>, 1999.
- 375 Hanslik, D., Jakobsson, M., Backman, J., Björck, S., Sellén, E., O’Regan, M., Fornaciari, E., and Skog, G.: Quaternary Arctic Ocean sea ice variations and radiocarbon reservoir age corrections, *Quaternary Science Reviews*, 29, 3430–3441, <https://doi.org/10.1016/j.quascirev.2010.06.011>, 2010.
- Hoerling, M. P., Hurrell, J. W., and Xu, T.: Tropical Origins for Recent North Atlantic Climate Change, 292, 90–92, <https://doi.org/10.1126/science.1058582>, 2001.
- 380 Holland, M. M. and Bitz, C. M.: Polar amplification of climate change in coupled models, *Climate Dynamics*, 21, 221–232, <https://doi.org/10.1007/s00382-003-0332-6>, 2003.
- Hurrell, J. W.: Decadal Trends in the North Atlantic Oscillation: Regional Temperatures and Precipitation, 269, 676–679, <https://doi.org/10.1126/science.269.5224.676>, 1995.
- 385 Jenkins, M. and Dai, A.: The Impact of Sea-Ice Loss on Arctic Climate Feedbacks and Their Role for Arctic Amplification, 48, e2021GL094599, <https://doi.org/10.1029/2021GL094599>, 2021.
- Johannessen, O. M., Bengtsson, L., Miles, M. W., Kuzmina, S. I., Semenov, V. A., Alekseev, G. V., Nagurnyi, A. P., Zakharov, V. F., Bobylev, L. P., Pettersson, L. H., Hasselmann, K., and Cattle, H. P.: Arctic climate change: observed and modelled temperature and sea-ice variability, 56, 328–341, <https://doi.org/10.3402/tellusa.v56i4.14418>, 2004.
- 390 Jones, P. D. and Moberg, A.: Hemispheric and Large-Scale Surface Air Temperature Variations: An Extensive Revision and an Update to 2001, 16, 206–223, [https://doi.org/10.1175/1520-0442\(2003\)016<0206:HALSSA>2.0.CO;2](https://doi.org/10.1175/1520-0442(2003)016<0206:HALSSA>2.0.CO;2), 2003.



- Jonkers, L., Cartapanis, O., Langner, M., McKay, N., Mulitza, S., Strack, A., and Kucera, M.: Integrating palaeoclimate time series with rich metadata for uncertainty modelling: strategy and documentation of the PalMod 130k marine palaeoclimate data synthesis, 12, 1053–1081, <https://doi.org/10.5194/essd-12-1053-2020>, 2020.
- 395 Joos, F. and Spahni, R.: Rates of change in natural and anthropogenic radiative forcing over the past 20,000 years, *PNAS*, 105, 1425–1430, <https://doi.org/10.1073/pnas.0707386105>, 2008.
- Kaufman, D., McKay, N., Routsou, C., Erb, M., Davis, B., Heiri, O., Jaccard, S., Tierney, J., Dätwyler, C., Axford, Y., Brussel, T., Cartapanis, O., Chase, B., Dawson, A., de Vernal, A., Engels, S., Jonkers, L., Marsicek, J., Moffa-Sánchez, P., Morrill, C., Orsi, A., Rehfeld, K., Saunders, K., Sommer, P. S., Thomas, E., Tonello, M., Tóth, M., Vachula, R., Andreev, A., Bertrand, S., Biskaborn, B., Bringué, M., Brooks, S., Caniupán, M., Chevalier, M., Cwynar, L., Emile-Geay, J., Fegyveresi, J., Feurdean, A., Finsinger, W., Fortin, M.-C., Foster, L., Fox, M., Gajewski, K., Grosjean, M., Hausmann, S., Heinrichs, M., Holmes, N., Ilyashuk, B., Ilyashuk, E., Juggins, S., Khider, D., Koinig, K., Langdon, P., Larocque-Tobler, I., Li, J., Lotter, A., Luoto, T., Mackay, A., Magyari, E., Malevich, S., Mark, B., Massaferró, J., Montade, V., Nazarova, L., Novenko, E., Pařil, P., Pearson, E., Peros, M., Pienitz, R., Plóciennik, M., Porinchu, D., Potito, A., Rees, A., Reinemann, S., Roberts, S., Rolland, N., Salonen, S., Self, A., Seppä, H., Shala, S., St-Jacques, J.-M., Stenni, B., Syrykh, L., Tarrats, P., Taylor, K., van den Bos, V., Velle, G., Wahl, E., Walker, I., Wilmshurst, J., Zhang, E., and Zhilich, S.: A global database of Holocene paleotemperature records, *Sci Data*, 7, 115, <https://doi.org/10.1038/s41597-020-0445-3>, 2020.
- 400 Kaufman, D. S., Ager, T. A., Anderson, N. J., Anderson, P. M., Andrews, J. T., Bartlein, P. J., Brubaker, L. B., Coats, L. L., Cwynar, L. C., Duvall, M. L., Dyke, A. S., Edwards, M. E., Eisner, W. R., Gajewski, K., Geirsdóttir, A., Hu, F. S., Jennings, A. E., Kaplan, M. R., Kerwin, M. W., Lozhkin, A. V., MacDonald, G. M., Miller, G. H., Mock, C. J., Oswald, W. W., Otto-Bliesner, B. L., Porinchu, D. F., Rühland, K., Smol, J. P., Steig, E. J., and Wolfe, B. B.: Holocene thermal maximum in the western Arctic (0–180°W), *Quaternary Science Reviews*, 23, 529–560, <https://doi.org/10.1016/j.quascirev.2003.09.007>, 2004.
- 405 Kaufman, D. S., Schneider, D. P., McKay, N. P., Ammann, C. M., Bradley, R. S., Briffa, K. R., Miller, G. H., Otto-Bliesner, B. L., Overpeck, J. T., Vinther, B. M., Arctic Lakes 2k Project Members, Abbott, M., Axford, Y., Bird, B., Birks, H. J. B., Bjune, A. E., Briner, J., Cook, T., Chipman, M., Francus, P., Gajewski, K., Geirsdóttir, Á., Hu, F. S., Kutchko, B., Lamoureux, S., Loso, M., MacDonald, G., Peros, M., Porinchu, D., Schiff, C., Seppä, H., and Thomas, E.: Recent Warming Reverses Long-Term Arctic Cooling, 325, 1236–1239, <https://doi.org/10.1126/science.1173983>, 2009.
- Kay, J. E., L’Ecuyer, T., Gettelman, A., Stephens, G., and O’Dell, C.: The contribution of cloud and radiation anomalies to the 2007 Arctic sea ice extent minimum, 35, <https://doi.org/10.1029/2008GL033451>, 2008.
- 420 Kirby, M. E., Lund, S. P., Patterson, W. P., Anderson, M. A., Bird, B. W., Ivanovici, L., Monarrez, P., and Nielsen, S.: A Holocene record of Pacific Decadal Oscillation (PDO)-related hydrologic variability in Southern California (Lake Elsinore, CA), *J Paleolimnol*, 44, 819–839, <https://doi.org/10.1007/s10933-010-9454-0>, 2010.
- Klein Goldewijk, K., Beusen, A., Doelman, J., and Stehfest, E.: Anthropogenic land use estimates for the Holocene – HYDE 3.2, 9, 927–953, <https://doi.org/10.5194/essd-9-927-2017>, 2017.



- 425 Kutzbach, J. E., Liu, X., Liu, Z., and Chen, G.: Simulation of the evolutionary response of global summer monsoons to orbital forcing over the past 280,000 years, *Clim Dyn*, 30, 567–579, <https://doi.org/10.1007/s00382-007-0308-z>, 2008.
- Larsen, N. K., Kjær, K. H., Lecavalier, B., Bjørk, A. A., Colding, S., Huybrechts, P., Jakobsen, K. E., Kjeldsen, K. K., Knudsen, K.-L., Odgaard, B. V., and Olsen, J.: The response of the southern Greenland ice sheet to the Holocene thermal maximum, *Geology*, 43, 291–294, <https://doi.org/10.1130/G36476.1>, 2015.
- 430 Lingfeng W., Jian L., Chaochao G., Weiyi S., Liang N., and Mi Y.: Study about influence of the Holocene volcanic eruptions on temperature variation trend by simulation, 40, 1597–1610, <https://doi.org/10.11928/j.issn.1001-7410.2020.06.19>, 2020.
- Liu, Z., Otto-Bliesner, B. L., He, F., Brady, E. C., Tomas, R., Clark, P. U., Carlson, A. E., Lynch-Stieglitz, J., Curry, W., Brook, E., Erickson, D., Jacob, R., Kutzbach, J., and Cheng, J.: Transient Simulation of Last Deglaciation with a New Mechanism for Bølling-Allerød Warming, 325, 310–314, <https://doi.org/10.1126/science.1171041>, 2009.
- 435 Liu, Z., Lu, Z., Wen, X., Otto-Bliesner, B. L., Timmermann, A., and Cobb, K. M.: Evolution and forcing mechanisms of El Niño over the past 21,000 years, 515, 550–553, <https://doi.org/10.1038/nature13963>, 2014.
- Lorenz, S. J. and Lohmann, G.: Acceleration technique for Milankovitch type forcing in a coupled atmosphere-ocean circulation model: method and application for the holocene, 23, 727–743, 2004.
- Mandel, I. and Lipovetsky, S.: Climate Change Report IPCC 2021 – A Chimera of Science and Politics, Social Science Research Network, Rochester, NY, <https://doi.org/10.2139/ssrn.3913788>, 2021.
- 440 Marcott, S. A., Shakun, J. D., Clark, P. U., and Mix, A. C.: A reconstruction of regional and global temperature for the past 11,300 years, *Science*, 339, 1198–1201, <https://doi.org/10.1126/science.1228026>, 2013.
- Marsicek, J., Shuman, B. N., Bartlein, P. J., Shafer, S. L., and Brewer, S.: Reconciling divergent trends and millennial variations in Holocene temperatures, 554, 92–96, <https://doi.org/10.1038/nature25464>, 2018.
- 445 Meyer, H., Opel, T., Laepple, T., Dereviagin, A. Y., Hoffmann, K., and Werner, M.: Long-term winter warming trend in the Siberian Arctic during the mid- to late Holocene, *Nature Geosci*, 8, 122–125, <https://doi.org/10.1038/ngeo2349>, 2015.
- Müller, J., Werner, K., Stein, R., Fahl, K., Moros, M., and Jansen, E.: Holocene cooling culminates in sea ice oscillations in Fram Strait, *Quaternary Science Reviews*, 47, 1–14, <https://doi.org/10.1016/j.quascirev.2012.04.024>, 2012.
- Niebauer, H. J., Bond, N., Yakunin, L. P., and Plotnikov, V.: An update on the climatology and sea ice of the Bering Sea, 1999.
- 450 Overland, J. E. and Wang, M.: Increased Variability in the Early Winter Subarctic North American Atmospheric Circulation, 28, 7297–7305, <https://doi.org/10.1175/JCLI-D-15-0395.1>, 2015.
- Park, H.-S., Kim, S.-J., Seo, K.-H., Stewart, A. L., Kim, S.-Y., and Son, S.-W.: The impact of Arctic sea ice loss on mid-Holocene climate, *Nat Commun*, 9, 4571, <https://doi.org/10.1038/s41467-018-07068-2>, 2018.
- Polyakov, I. V. and Johnson, M. A.: Arctic decadal and interdecadal variability, 27, 4097–4100, <https://doi.org/10.1029/2000GL011909>, 2000.
- 455 Polyakov, I. V., Alekseev, G. V., Bekryaev, R. V., Bhatt, U., Colony, R. L., Johnson, M. A., Karklin, V. P., Makshtas, A. P., Walsh, D., and Yulin, A. V.: Observationally based assessment of polar amplification of global warming, 29, 25-1-25-4, <https://doi.org/10.1029/2001GL011111>, 2002.



- Ragner, C.: The 21st Century — Turning Point for the Northern Sea Route?: Proceedings of the Northern Sea Route User
460 Conference, Oslo, 18–20 November 1999, <https://doi.org/10.1007/978-94-017-3228-4>, 2000.
- Rahmstorf, S.: Shifting seas in the greenhouse?, 399, 523–524, <https://doi.org/10.1038/21066>, 1999.
- Renssen, H., Goosse, H., Fichefet, T., Brovkin, V., Driesschaert, E., Wolk, F., and Climate Change and Landscape Dynamics:
Simulating the Holocene climate evolution at northern high latitudes using a coupled atmosphere-sea ice-ocean-vegetation
model, 24, 23–43, <https://doi.org/10.1007/s00382-004-0485-y>, 2005.
- 465 Renssen, H., Seppä, H., Crosta, X., Goosse, H., and Roche, D. M.: Global characterization of the Holocene Thermal Maximum,
Quaternary Science Reviews, 48, 7–19, <https://doi.org/10.1016/j.quascirev.2012.05.022>, 2012.
- Rodionov, S. N., Overland, J. E., and Bond, N. A.: The Aleutian Low and Winter Climatic Conditions in the Bering Sea. Part
I: Classification, 18, 160–177, <https://doi.org/10.1175/JCLI3253.1>, 2005.
- Routson, C. C., McKay, N. P., Kaufman, D. S., Erb, M. P., Goosse, H., Shuman, B. N., Rodysill, J. R., and Ault, T.: Mid-
470 latitude net precipitation decreased with Arctic warming during the Holocene, 568, 83–87, <https://doi.org/10.1038/s41586-019-1060-3>, 2019.
- Screen, J. A.: Far-flung effects of Arctic warming, *Nature Geosci*, 10, 253–254, <https://doi.org/10.1038/ngeo2924>, 2017.
- Screen, J. A. and Simmonds, I.: Amplified mid-latitude planetary waves favour particular regional weather extremes, *Nature
Clim Change*, 4, 704–709, <https://doi.org/10.1038/nclimate2271>, 2014.
- 475 Serreze, M. C. and Barry, R. G.: Processes and impacts of Arctic amplification: A research synthesis, *Global and Planetary
Change*, 77, 85–96, <https://doi.org/10.1016/j.gloplacha.2011.03.004>, 2011.
- Sigl, M., Winstrup, M., McConnell, J. R., Welten, K. C., Plunkett, G., Ludlow, F., Büntgen, U., Caffee, M., Chellman, N.,
Dahl-Jensen, D., Fischer, H., Kipfstuhl, S., Kostick, C., Maselli, O. J., Mekhaldi, F., Mulvaney, R., Muscheler, R., Pasteris, D.
R., Pilcher, J. R., Salzer, M., Schüpbach, S., Steffensen, J. P., Vinther, B. M., and Woodruff, T. E.: Timing and climate forcing
480 of volcanic eruptions for the past 2,500 years, 523, 543–549, <https://doi.org/10.1038/nature14565>, 2015.
- Smith, D. M., Screen, J. A., Deser, C., Cohen, J., Fyfe, J. C., García-Serrano, J., Jung, T., Kattsov, V., Matei, D., Msadek, R.,
Peings, Y., Sigmond, M., Ukita, J., Yoon, J.-H., and Zhang, X.: The Polar Amplification Model Intercomparison Project
(PAMIP) contribution to CMIP6: investigating the causes and consequences of polar amplification, 12, 1139–1164,
<https://doi.org/10.5194/gmd-12-1139-2019>, 2019.
- 485 Smith, R. S. and Gregory, J.: The last glacial cycle: transient simulations with an AOGCM, *Clim Dyn*, 38, 1545–1559,
<https://doi.org/10.1007/s00382-011-1283-y>, 2012.
- Stabeno, P. J., Bond, N. A., Kachel, N. B., Salo, S. A., and Schumacher, J. D.: On the temporal variability of the physical
environment over the south-eastern Bering Sea, 10, 81–98, <https://doi.org/10.1046/j.1365-2419.2001.00157.x>, 2001.
- Sundqvist, H. S., Kaufman, D. S., McKay, N. P., Balascio, N. L., Briner, J. P., Cwynar, L. C., Sejrup, H. P., Seppä, H., Subetto,
490 D. A., Andrews, J. T., Axford, Y., Bakke, J., Birks, H. J. B., Brooks, S. J., de Vernal, A., Jennings, A. E., Ljungqvist, F. C.,
Rühland, K. M., Saenger, C., Smol, J. P., and Viau, A. E.: Arctic Holocene proxy climate database – new approaches



- to assessing geochronological accuracy and encoding climate variables, 10, 1605–1631, <https://doi.org/10.5194/cp-10-1605-2014>, 2014.
- 495 Timm, O. and Timmermann, A.: Simulation of the Last 21 000 Years Using Accelerated Transient Boundary Conditions*, 20, 4377–4401, <https://doi.org/10.1175/JCLI4237.1>, 2007.
- Timmermann, A., Friedrich, T., Timm, O. E., Chikamoto, M. O., Abe-Ouchi, A., and Ganopolski, A.: Modeling Obliquity and CO₂ Effects on Southern Hemisphere Climate during the Past 408 ka, 27, 1863–1875, <https://doi.org/10.1175/JCLI-D-13-00311.1>, 2014.
- 500 Vavrus, S. J.: The Influence of Arctic Amplification on Mid-latitude Weather and Climate, *Curr Clim Change Rep*, 4, 238–249, <https://doi.org/10.1007/s40641-018-0105-2>, 2018.
- Vieira, L. E. A., Solanki, S. K., Krivova, N. A., and Usoskin, I.: Evolution of the solar irradiance during the Holocene, *A&A*, 531, A6, <https://doi.org/10.1051/0004-6361/201015843>, 2011.
- Wang, B., Zhou, T., and Yu, Y.: A perspective on Earth system model development, 66(6), 857–869, 2008.
- 505 Wang, Z., Liu, J., Wang, X., and Liu, B.: Divergent sensitivity of Earth System Model CESM1. 0 to solar radiation versus greenhouse gases, 36(3), 758–767, 2016.
- Wang, Z., Wang, J., Zhang, S., LI, K., Zuo, R., and Liujian: Impact of different timescales on the characteristics and mechanisms of the Northern Hemisphere Summer Monsoon Based on the CESM results, 38(6):, 1494–1506., 2018.
- Wanner, H., Solomina, O., Grosjean, M., Ritz, S. P., and Jetel, M.: Structure and origin of Holocene cold events, *Quaternary Science Reviews*, 30, 3109–3123, <https://doi.org/10.1016/j.quascirev.2011.07.010>, 2011.
- 510 Watanabe, E., Wang, J., Sumi, A., and Hasumi, H.: Arctic dipole anomaly and its contribution to sea ice export from the Arctic Ocean in the 20th century, 33, <https://doi.org/10.1029/2006GL028112>, 2006.
- Wohlfahrt, J., Harrison, S. P., and Braconnot, P.: Synergistic feedbacks between ocean and vegetation on mid- and high-latitude climates during the mid-Holocene, 22, 223–238, <https://doi.org/10.1007/s00382-003-0379-4>, 2004.
- 515 Wu, B., Wang, J., and Walsh, J.: Possible Feedback of Winter Sea Ice in the Greenland and Barents Seas on the Local Atmosphere, 132, 1868–1876, [https://doi.org/10.1175/1520-0493\(2004\)132<1868:PFOWSI>2.0.CO;2](https://doi.org/10.1175/1520-0493(2004)132<1868:PFOWSI>2.0.CO;2), 2004.
- Wu, B., Wang, J., and Walsh, J. E.: Dipole Anomaly in the Winter Arctic Atmosphere and Its Association with Sea Ice Motion, 19, 210–225, <https://doi.org/10.1175/JCLI3619.1>, 2006.
- Xue, D., Lu, J., Sun, L., Chen, G., and Zhang, Y.: Local increase of anticyclonic wave activity over northern Eurasia under amplified Arctic warming, 44, 3299–3308, <https://doi.org/10.1002/2017GL072649>, 2017.
- 520 Zheng, P., Song, J., Zhang, F., and Bao, X.: Common instruction of some OGCM, 25 (4), 108–120, 2008.
- Zhong, Y., Jahn, A., Miller, G. H., and Geirsdottir, A.: Asymmetric Cooling of the Atlantic and Pacific Arctic During the Past Two Millennia: A Dual Observation-Modeling Study, *Geophys. Res. Lett.*, 45, <https://doi.org/10.1029/2018GL079447>, 2018.